

# Robustness of Contraction Metrics Computed by Radial Basis Functions

Peter Giesl<sup>1</sup><sup>a</sup>, Sigurdur Hafstein<sup>2</sup><sup>b</sup> and Iman Mehrabinezhad<sup>2</sup><sup>c</sup>

<sup>1</sup>Department of Mathematics, University of Sussex, Falmer BN1 9QH, U.K.

<sup>2</sup>Faculty of Physical Sciences, University of Iceland, Dunhagi 5, IS-107 Reykjavik, Iceland

Keywords: Contraction Metric, Radial Basis Functions, Periodic Orbits, Dynamical System.

Abstract: We study contraction metrics computed for dynamical systems with periodic orbits using generalized interpolation with radial basis functions. The robustness of the metric with respect to perturbations of the system is proved and demonstrated for two examples from the literature.

## 1 INTRODUCTION

Consider an autonomous ordinary differential equation (ODE) of the form

$$\dot{\mathbf{x}} = \mathbf{f}(\mathbf{x}), \quad \mathbf{x} \in \mathbb{R}^n \quad (1)$$

with a  $C^s$ -vector field  $\mathbf{f}: \mathbb{R}^n \rightarrow \mathbb{R}^n$  with  $s \geq 1$ . The existence, uniqueness, and stability of periodic orbits in a given area can be investigated using a Riemannian contraction metric. Further, their basins of attraction can be rigorously estimated. A contraction metric is a local criterion that does not require knowledge of the precise location of the periodic orbit and it is robust to small perturbations of the system. This means that a contraction metric for (1) remains a contraction metric for a perturbed system, even with a perturbed periodic orbit.

A contraction metric provides a local criterion to compare the evolution of two trajectories – this idea is also used for the related notions of incremental stability, i.e. the stability between two adjacent solutions, and convergent systems, i.e. systems converging to a unique solution as time tends to infinity. For a detailed comparison of these notions, also in non-autonomous systems, see (Rüffer et al., 2013) and (Fromion and Scorletti, 2005). Incremental stability was studied in (Lohmiller and Slotine, 1998) and (Angeli, 2002). The related notion of Finsler-Lyapunov functions was introduced by (Forni and Sepulchre, 2014). The study of contraction metrics in general goes back to (Lewis, 1949; Opial, 1960; Demidovič, 1961; Demidovič,

1967). The review (Jouffroy, 2005) puts the definition from (Lohmiller and Slotine, 1998) into historical context.

Contraction metrics for periodic orbits have been considered by (Borg, 1960) with the Euclidean metric and (Stenström, 1962) with a general Riemannian metric. They have also been studied in (Hartman and Olech, 1962; Hartman, 1964; Krasovskii, 1963; Kravchuk et al., 1992; Leonov et al., 1996).

For periodic orbits, the notions of Zhukovskii stability, see e.g. (Leonov et al., 2001), i.e. stability of solutions after reparameterisation of time, has been used to study stability. The reparameterisation or synchronisation of the time of adjacent trajectories is used to show that the existence of a contraction metric implies the existence of a unique, exponentially stable periodic orbit to which all trajectories converge, see (Yang, 2001) or (Manchester and Slotine, 2014). Converse theorems to prove the existence of a Riemannian contraction metric for a system with an exponentially stable periodic orbit go back to (Hauser and Chung, 1994), where a local version is proved, and (Manchester and Slotine, 2014), where a global version on a compact sets is proved. The latter also discusses the robustness to parameters, using the construction in (Leonov, 2006).

(Giesl, 2020) contains a global converse theorem, showing the existence of a contraction metric on the entire phase space for systems with an exponentially stable periodic orbit. The metric was characterized as the solution of a linear matrix-valued PDE and an existence and uniqueness theorem was proved. In (Giesl, 2019) a numerical method using generalized interpolation with radial basis functions (RBFs) to compute such a contraction metric was presented. In

<sup>a</sup>  <https://orcid.org/0000-0003-1421-6980>

<sup>b</sup>  <https://orcid.org/0000-0003-0073-2765>

<sup>c</sup>  <https://orcid.org/0000-0002-6346-9901>

(Giesl et al., 2021b) we presented a rigorous verification of the properties of a contraction metric for the metric computed in (Giesl, 2019) and showed that the combination delivers a method that is able to compute and verify a contraction metric for any system with an exponentially stable periodic orbit. In this paper, we focus on a perturbation of the system and its effect with respect to the construction and verification of the contraction metric computed by our method. Finally, we present two examples to illustrate the theoretical result.

The main idea of the procedure in (Giesl et al., 2021b) is similar to (Giesl et al., 2021a), in which we provided a computation and verification method for contraction metrics in the case of exponentially stable equilibria. As in (Giesl et al., 2021a) we showed that the method is successful in computing a metric if sufficiently many collocation points are used in the computation in (Giesl, 2019) and sufficiently small simplices in the verification. However, in contrast to the case of an equilibrium, the contraction condition for periodic orbits involves the restriction to the  $(n-1)$ -dimensional subspace perpendicular to  $\mathbf{f}(\mathbf{x})$  at each point  $\mathbf{x}$ , which required a more sophisticated argumentation.

Computational methods for contraction metrics have been proposed in (Giesl and Hafstein, 2013) for periodic orbits in time-periodic systems, where the contraction metric was a continuous piecewise affine (CPA) function and the contraction conditions were transformed into constraints of a semidefinite optimization problem. In (Manchester and Slotine, 2014, Theorem 3) a contraction metric for periodic orbits was constructed using Linear Matrix Inequalities and SOS (sum of squares). While both of these methods also include a rigorous verification, similar to our approach, they are of higher computational complexity because they require solving a semidefinite optimization problem, whereas solving a system of linear equations is computationally the most demanding step in the approach from (Giesl et al., 2021b).

## 2 SUMMARY OF THE METHOD

In this section, we briefly review contraction metrics for periodic orbits and the method from (Giesl et al., 2021b); more details on both can be found in (Giesl et al., 2021b). We first need a few definitions.

**Definition 2.1** (Riemannian/contraction metric). *Let  $G$  be an open subset of  $\mathbb{R}^n$ . A Riemannian metric is a locally Lipschitz continuous matrix-valued function  $M : G \rightarrow \mathbb{S}^{n \times n}$ , such that  $M(\mathbf{x})$  is positive definite for all  $\mathbf{x} \in G$ , where  $\mathbb{S}^{n \times n}$  denotes the sym-*

*metric  $n \times n$  matrices with real entries.*

*A contraction metric for a periodic orbit is a Riemannian metric  $M : G \rightarrow \mathbb{S}^{n \times n}$  fulfilling a contraction condition expressed by  $L_M(\mathbf{x}) \leq -\nu < 0$  for all  $\mathbf{x} \in K \subset G$ , where  $L_M$  is defined in (3) below and  $K$  is a compact subset of the open set  $G \subset \mathbb{R}^n$  such that  $\mathbf{f}(\mathbf{x}) \neq 0$  holds for all  $\mathbf{x} \in K$ . For the definition of  $L_M$  we first define for all  $\mathbf{x} \in \mathbb{R}^n$  with  $\mathbf{f}(\mathbf{x}) \neq 0$*

$$V(\mathbf{x}) = D\mathbf{f}(\mathbf{x}) - \frac{\mathbf{f}(\mathbf{x})\mathbf{f}(\mathbf{x})^T(D\mathbf{f}(\mathbf{x}) + D\mathbf{f}(\mathbf{x})^T)}{\|\mathbf{f}(\mathbf{x})\|_2^2}. \quad (2)$$

*For all  $\mathbf{x} \in \mathbb{R}^n$  with  $\mathbf{f}(\mathbf{x}) \neq 0$  we define*

$$L_M(\mathbf{x}) = \max_{\mathbf{v} \in \mathbb{R}^n, \mathbf{v}^T M(\mathbf{x})\mathbf{v} = 1, \mathbf{v}^T \mathbf{f}(\mathbf{x}) = 0} L_M(\mathbf{x}; \mathbf{v}) \quad \text{where} \quad (3)$$

$$L_M(\mathbf{x}; \mathbf{v}) = \frac{1}{2} \mathbf{v}^T \left( M'_+(\mathbf{x}) + V(\mathbf{x})^T M(\mathbf{x}) + M(\mathbf{x}) V(\mathbf{x}) \right) \mathbf{v}.$$

*The forward orbital derivative  $M'_+(\mathbf{x})$  with respect to (1) at  $\mathbf{x} \in G$  is defined by*

$$M'_+(\mathbf{x}) := \limsup_{h \rightarrow 0^+} \frac{M(S_h \mathbf{x}) - M(\mathbf{x})}{h} \quad (4)$$

*where  $t \mapsto S_t \mathbf{x}$  is the solution to (1) passing through  $\mathbf{x}$  at time  $t = 0$ . We refer to  $M$  as a (Riemannian) contraction metric on  $K$  or a metric contracting in  $K$ .*

The function  $L_M(\mathbf{x}; \mathbf{v})$  in (3) above is negative for  $\mathbf{v}$  with  $\mathbf{v}^T \mathbf{f}(\mathbf{x}) = 0$ , if for small  $\delta > 0$  the distance between solutions through  $\mathbf{x}$  and  $\mathbf{x} + \delta \mathbf{v}$  decreases with respect to the metric  $M(\mathbf{x})$ . For a heuristic explanation of this fact, see, e.g. (Giesl, 2019, Section 1).

Two theorems reveal the connection between periodic orbits and contraction metrics. (Giesl et al., 2021b, Theorem 2.5) shows that the existence of a contraction metric on a compact, forward invariant set  $K$  asserts the existence of a unique exponentially stable periodic orbit  $\Omega \subset K$  and that  $K$  is a subset of the orbit's basin of attraction, i.e.  $K \subset \mathcal{A}(\Omega)$ . Conversely, (Giesl, 2020, Theorems 3.1, 4.2) establish the existence of a contraction metric for exponentially stable periodic orbits, as the solution to a matrix-valued PDE. In order to explain this in more detail, we first need to define for all  $\mathbf{x} \in \mathbb{R}^n$  with  $\mathbf{f}(\mathbf{x}) \neq 0$  the linear differential operator  $L$ , acting on  $M \in C^0(\mathbb{R}^n; \mathbb{S}^{n \times n})$  by

$$LM(\mathbf{x}) := M'_+(\mathbf{x}) + V(\mathbf{x})^T M(\mathbf{x}) + M(\mathbf{x}) V(\mathbf{x}), \quad (5)$$

where  $V$  was defined in (2). Moreover, we define the projection  $P_{\mathbf{x}}$  for all  $\mathbf{x} \in \mathbb{R}^n$  with  $\mathbf{f}(\mathbf{x}) \neq 0$  onto the  $(n-1)$ -dimensional space perpendicular to  $\mathbf{f}(\mathbf{x})$ , i.e.  $P_{\mathbf{x}}^2 = P_{\mathbf{x}}$ ,  $P_{\mathbf{x}} \mathbf{f}(\mathbf{x}) = 0$  and  $P_{\mathbf{x}} \mathbf{v} = \mathbf{v}$  if  $\mathbf{v}^T \mathbf{f}(\mathbf{x}) = 0$ , by

$$P_{\mathbf{x}} := I_{n \times n} - \frac{\mathbf{f}(\mathbf{x})\mathbf{f}(\mathbf{x})^T}{\|\mathbf{f}(\mathbf{x})\|_2^2}. \quad (6)$$

Then for  $B \in C^{s-1}(\mathcal{A}(\Omega); \mathbb{S}^{n \times n})$  such that  $B(\mathbf{x})$  is positive definite for all  $\mathbf{x} \in \mathcal{A}(\Omega)$ , we define  $C \in C^{s-1}(\mathcal{A}(\Omega); \mathbb{S}^{n \times n})$  by

$$C(\mathbf{x}) = P_{\mathbf{x}}^T B(\mathbf{x}) P_{\mathbf{x}}. \quad (7)$$

(Giesl, 2020, Theorems 3.1 and 4.2) assert that there exists a unique solution  $M \in C^{s-1}(\mathcal{A}(\Omega); \mathbb{S}^{n \times n})$  of the linear matrix-valued PDE

$$LM(\mathbf{x}) = -C(\mathbf{x}) \text{ for all } \mathbf{x} \in \mathcal{A}(\Omega) \quad (8)$$

$$\text{satisfying } \mathbf{f}(\mathbf{x}_0)^T M(\mathbf{x}_0) \mathbf{f}(\mathbf{x}_0) = c_0 \|\mathbf{f}(\mathbf{x}_0)\|_2^4, \quad (9)$$

where  $\mathbf{x}_0 \in \mathcal{A}(\Omega)$  and  $c_0 \in \mathbb{R}^+$  are fixed. The first step of the method in (Giesl et al., 2021b) to rigorously compute a contraction metric is to follow (Giesl, 2020) and solve the PDE (8) numerically using RBFs to obtain a contraction metric that can be computed knowing the values  $LM(\mathbf{x}_i)$  at finitely many collocation points  $\mathbf{x}_i$  within a set  $O$ . This procedure is referred to as a generalized interpolation problem or the optimal recovery problem, because it produces a function  $S$  fulfilling  $LS(\mathbf{x}_i)$  that is norm minimal in the corresponding reproducing kernel Hilbert space (RKHS). The existence and uniqueness of the optimal recovery has been proved in (Giesl, 2019, Theorem 4.2) and error estimates for the RBF approximation have been obtained in (Giesl, 2019, Theorem 4.4). While this theorem provides a proof that the RBF approximation  $S$  to  $M$  is a contraction metric if the so-called *fill distance*  $h_{X,O}$  of the set of collocation points  $X$  in  $O$  is small enough, it does not quantify in a useful way how small  $h_{X,O}$  must be because unknown constants appear in the estimate. This is why we need a verification method that allows us to check whether  $S$  is a contraction metric or whether we need add collocation points to make  $h_{X,O}$  smaller.

Thus, in the second step of the method from (Giesl et al., 2021b) the conditions for a contraction metric are rigorously verified for the CPA interpolation  $P$  of the contraction metric  $S$ , which was computed in the first step. In particular, it is verified that  $P(\mathbf{x})$  is positive definite and  $L_P(\mathbf{x})$  is negative definite for all  $\mathbf{x} \in \mathcal{D}_{\mathcal{T}}^o$ , see (Giesl et al., 2021b, Theorem 4.11), where  $\mathcal{D}_{\mathcal{T}}$  is the area triangulated by the triangulation  $\mathcal{T}$ . In (Giesl et al., 2021b) error estimates and statements about the CPA interpolation are provided, together with criteria that assert that the interpolation is a contraction metric itself. The essential point is that these criteria can be verified numerically very efficiently.

To be more precise, given a system  $\dot{\mathbf{x}} = \mathbf{f}(\mathbf{x})$ ,  $\mathbf{f} \in C^3(\mathbb{R}^n; \mathbb{R}^n)$ , and a finite triangulation  $\mathcal{T} = \bigcup_{\mathfrak{S}_v} \mathfrak{S}_v$  of  $\mathcal{D}_{\mathcal{T}} \subset \mathbb{R}^n$  with vertex set  $\mathbf{x}_k \in \mathcal{V}_{\mathcal{T}}$ , such that  $\mathbf{f}(\mathbf{x}) \neq 0$  for all  $\mathbf{x} \in \mathcal{D}_{\mathcal{T}}$ , we need to check the following constraints:

**(VP1) Positive definiteness of P**

For each vertex  $\mathbf{x}_k \in \mathcal{V}_{\mathcal{T}}$   $P(\mathbf{x}_k)$  is positive definite, i.e. :

$$P(\mathbf{x}_k) \succ 0_{n,n}.$$

**(VP2) Negative definiteness of  $A_v - \kappa_v^* \mathbf{f} \mathbf{f}^T$**

For each simplex  $\mathfrak{S}_v = \text{co}(\mathbf{x}_0, \dots, \mathbf{x}_n) \in \mathcal{T}$  (convex hull) and each vertex  $\mathbf{x}_k$  of  $\mathfrak{S}_v$  :

$$A_v(\mathbf{x}_k) - \kappa_v^* \mathbf{f}(\mathbf{x}_k) \mathbf{f}^T(\mathbf{x}_k) + h_v^2 E_v I_{n \times n} \prec 0_{n,n}.$$

Here

$$A_v(\mathbf{x}_k) := P(\mathbf{x}_k) V(\mathbf{x}_k) + V(\mathbf{x}_k)^T P(\mathbf{x}_k) + \left( \nabla P_{ij}^y \cdot \mathbf{f}(\mathbf{x}_k) \right)_{i,j=1,2,\dots,n}, \quad (10)$$

where  $\kappa_v^*$ , and  $E_v$  are tailored constants for the system for each simplex  $\mathfrak{S}_v \in \mathcal{T}$ , and  $h_v$  is its diameter  $h_v := \text{diam}(\mathfrak{S}_v) = \max_{\mathbf{x}, \mathbf{y} \in \mathfrak{S}_v} \|\mathbf{x} - \mathbf{y}\|_2$ .

Our verification problem is a semidefinite feasibility problem and can in theory be solved as such. However, it is computationally much more efficient to assign values to the variables  $P(\mathbf{x}_k)$  of the problem using the optimal recovery  $S$  of the solution to (8) and (9), i.e.  $P(\mathbf{x}_k) = S(\mathbf{x}_k)$ , and then verify that the constraints of the feasibility problem are fulfilled. We will refer to this feasibility problem as *verification problem*. A contraction metric  $M$  for the system (1) will also be a contraction metric for a perturbed system, as shown in the next theorem. To quantify perturbations we define for  $W \in C^k(\mathcal{D}; \mathcal{R})$ , where  $\mathcal{D} \subset \mathbb{R}^n$  is a non-empty open set and  $\mathcal{R}$  is  $\mathbb{R}, \mathbb{R}^n, \mathbb{S}^{n \times n}$ , or  $\mathbb{R}^{n \times n}$ , the  $C^k$ -norm as

$$\|W\|_{C^k(\mathcal{D}; \mathcal{R})} := \sum_{|\alpha| \leq k} \sup_{\mathbf{x} \in \mathcal{D}} \|D^\alpha W(\mathbf{x})\|_2.$$

In this formula  $\alpha \in \mathbb{N}_0^n$  is a multi-index and  $|\alpha| = \sum_{i=1}^n \alpha_i$ .

**Theorem 2.2.** *Assume that  $M : G \rightarrow \mathbb{S}^{n \times n}$  is a contraction metric as in Definition 2.1 for system (1), where  $\mathbf{f}$  is  $C^1$ , and contracting in the compact set  $K \subset G$ . Then there is an  $\varepsilon > 0$  such that  $M : G \rightarrow \mathbb{S}^{n \times n}$  is also a contraction metric for any perturbed system  $\dot{\mathbf{x}} = \tilde{\mathbf{f}}(\mathbf{x})$ , where  $\tilde{\mathbf{f}}$  is  $C^1$  and  $\|\tilde{\mathbf{f}} - \mathbf{f}\|_{C^1(G; \mathbb{R}^n)} < \varepsilon$ .*

*Proof.* By assumption  $M(\mathbf{x})$  is symmetric and positive definite for every  $\mathbf{x} \in G \subset \mathbb{R}^n$ . Hence, we only need to verify that  $L_M(\mathbf{x}) < 0$  holds true for all  $\mathbf{x} \in K$  when  $\mathbf{f}$  has been substituted by  $\tilde{\mathbf{f}}$  in (2), (3), and (4).

We choose  $\varepsilon > 0$  so small that  $\tilde{\mathbf{f}}(\mathbf{x}) \neq 0$  for all  $\mathbf{x} \in K$ . Then we note, that the right-hand side of formula (2) is a continuous function of  $\mathbf{y} = \mathbf{f}(\mathbf{x})$  and  $Z = D\mathbf{f}(\mathbf{x})$ . Thus  $V(\mathbf{x})$  varies continuously when  $\mathbf{f}$  is substituted by  $\tilde{\mathbf{f}}$  with  $\|\tilde{\mathbf{f}} - \mathbf{f}\|_{C^1(G; \mathbb{R}^n)} < \varepsilon$ . To see

that (4) varies continuously we recall standard results on the continuous dependence of solutions to ODE, e.g. (Walter, 1998, §12.V), which implies that from  $\|\tilde{\mathbf{f}} - \mathbf{f}\|_{C^1(G; \mathbb{R}^n)} < \varepsilon$  follows

$$\|\tilde{S}_h \mathbf{x} - S_h \mathbf{x}\|_2 \leq \frac{\varepsilon}{L} (e^{Lh} - 1),$$

where  $S_h \mathbf{x}$  and  $\tilde{S}_h \mathbf{x}$  are the solutions at time  $h > 0$ , starting at  $\mathbf{x} \in K$  to  $\dot{\mathbf{x}} = \mathbf{f}(\mathbf{x})$  and  $\dot{\mathbf{x}} = \tilde{\mathbf{f}}(\mathbf{x})$  respectively, and the solution trajectories are in an open set  $O$ ,  $K \subset O \subset \bar{O} \subset G$ , and  $\bar{O}$  is compact. Further,  $0 < L < \infty$  is a Lipschitz constant for  $\mathbf{f}$  in  $\bar{O}$ .

Let  $0 < L^* < \infty$  be a Lipschitz constant for  $M$  on  $\bar{O}$  with respect to the  $\|\cdot\|_2$  norm. Then we have

$$\left\| \frac{M(\tilde{S}_h \mathbf{x}) - M(\mathbf{x})}{h} - \frac{M(S_h \mathbf{x}) - M(\mathbf{x})}{h} \right\|_2 = \frac{L^*}{h} \|\tilde{S}_h \mathbf{x} - S_h \mathbf{x}\|_2 \leq L^* \varepsilon \frac{e^{Lh} - 1}{Lh} \leq 2L^* \varepsilon$$

for small enough  $h > 0$ . Thus  $M'_+(\mathbf{x})$  also varies continuously when  $\mathbf{f}$  is substituted by  $\tilde{\mathbf{f}}$  with  $\|\tilde{\mathbf{f}} - \mathbf{f}\|_{C^1(G; \mathbb{R}^n)} < \varepsilon$  and we have established that  $L_M(\mathbf{x}; \mathbf{v})$  varies continuously. The assertion now follows from the fact that both the argument of the maximum in (3) and the set maximized over, an intersection of an ellipsoid with a hyper-plane, vary continuously when  $\mathbf{f}$  is substituted by  $\tilde{\mathbf{f}}$  with  $\|\tilde{\mathbf{f}} - \mathbf{f}\|_{C^1(G; \mathbb{R}^n)} < \varepsilon$ , because neither  $\mathbf{f}(\mathbf{x}) = 0$  nor  $\tilde{\mathbf{f}}(\mathbf{x}) = 0$  on  $K$ . Thus  $L_M(\mathbf{x}) < 0$  remains true after the substitution if  $\varepsilon > 0$  is small enough.  $\square$

This robustness property is a very desired property in dynamical systems. Note also that one could even prove that (VP1) and (VP2) of the verification remain true after a small perturbation, but then one must demand that  $\mathbf{f}, \tilde{\mathbf{f}}$  are  $C^3$  and that  $\|\tilde{\mathbf{f}} - \mathbf{f}\|_{C^2(G; \mathbb{R}^n)} < \varepsilon$  because the constants  $E_v$  in (VP2) depend on the second derivatives of the right-hand side of the system (1).

A short discussion of the numerical complexity of our method follows: The number of elementary arithmetic operations needed for computing the coefficients of the collocation matrix in the RBF-step is of the order  $O(N^2)$  for a fixed  $n$ , where  $N$  is the number of collocation points and  $n$  is the dimension of the system. The order in  $n$  for a fixed  $N$  is at least  $O(n^5)$ ; depending on  $f$  and  $Df$  it might be higher. To solve the linear equations  $O((Nn^2)^3) = O(N^3n^6)$  elementary operations are needed. Typically  $N \gg n$  and therefore the complexity of the first step of the algorithm is  $O(N^3n^6)$ , where we consider the dimension  $n$  of the system to be fixed.

In the second step of the method, we first evaluate  $P(\cdot)$  at every vertex of the triangulation. For each

vertex we need  $O(N)$  elementary operations for this, again ignoring the dependence on  $n$ . Then we verify the constraints (VP1)-(VP2). Since this must be done for every vertex we need at least  $O(N_{CPA}N)$  operations, where  $N_{CPA}$  denotes the number of vertices of the triangulation.

Clearly, the number of simplices in the triangulation is bounded above by  $N_{CPA}n!$ . Therefore, the complexity of the verification of the constraints (VP1)-(VP2) is linear in  $N_{CPA}$  and independent of  $N$ . Thus, the numerical complexity of the second step of the method is  $O(N_{CPA}N)$ , again assuming a fixed dimension  $n$ . However, note that the computational effort grows very fast with the dimension  $n$  of the system, in particular since  $N$  and  $N_{CPA}$  can be expected to grow exponentially with the dimension (curse of dimensionality).

In the next section we demonstrate the applicability of our theoretical results to two examples. Note that the periodic orbit is displayed in the figures through a numerical approximation for comparison in orange, but the method verifies rigorously that it exists and is exponentially stable and, moreover, determines a subset of its basin of attraction.

### 3 EXAMPLES

We implemented our method in C++ and ran the examples on an AMD Ryzen 2700X processor with 8 cores at 3.7 GHz and with 64GB RAM. In order to compute a positively invariant set  $K$  for the dynamical systems  $\dot{\mathbf{x}} = \mathbf{f}(\mathbf{x})$  we use a procedure motivated by (Giesl and Hafstein, 2015). First we solve numerically the PDE

$$\sum_{i=1}^n \frac{\partial V}{\partial x_i}(\mathbf{x}) f_i(\mathbf{x}) = \nabla V(\mathbf{x}) \cdot \mathbf{f}(\mathbf{x}) = -\sqrt{\delta^2 + \|\mathbf{f}(\mathbf{x})\|_2^2}, \quad (11)$$

with  $\delta = 10^{-8}$ , using RBF. Then we use CPA interpolation  $V_P$  of the numerical solution and verify where  $\nabla V_P(\mathbf{x}) \cdot \mathbf{f}(\mathbf{x}) < 0$  holds true. In this area the function  $V_P$  is decreasing along solution trajectories and a sublevel set  $\{\mathbf{x} \in \mathbb{R}^n : V_P(\mathbf{x}) \leq c\}$  is necessarily forward invariant, if its boundary is fully contained in this area. Hence, we only need  $\nabla V_P(\mathbf{x}) \cdot \mathbf{f}(\mathbf{x}) < 0$  on the level set  $\{\mathbf{x} \in \mathbb{R}^n : V_P(\mathbf{x}) = c\}$ , not on the whole sublevel set. We refer to  $V_P$  as *Lyapunov-like function*.

The *failing points* of the Lyapunov-like function (see for example Figure 2) are the points where the function  $V_P$  is not decreasing along solution trajectories. In order to obtain a positively invariant set, we need to

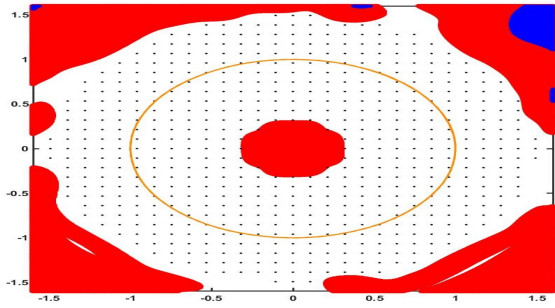


Figure 1: Example 3.1. The black dots show the collocation points and the orange curve is the periodic orbit for system (12). We plot the area where the constraints of Verification Problem fail to be fulfilled; in blue if (VP1) is violated and in red if (VP2) is violated. Where neither is violated (white), the CPA interpolation  $P$  fulfills the properties of a contraction metric.

find a sublevel set of the function such that its boundary does contain any of these points.

### 3.1 Unit Circle

As a first example, we consider the following system

$$\begin{cases} \dot{x} &= x(1-x^2-y^2)-y \\ \dot{y} &= y(1-x^2-y^2)+x \end{cases} \quad (12)$$

of which the unit circle is an exponentially stable periodic orbit and the origin is an unstable equilibrium. We choose  $B(\mathbf{x}) = I_{2 \times 2}$  and the collocation points  $X = \frac{1}{15}\mathbb{Z}^2 \cap \{(x,y) \in \mathbb{R}^2 : 0.25 < \sqrt{x^2+y^2} < 1.5\}$  as well as the point  $\mathbf{x}_0 = (1,0)$  with  $c_0 = 1$ . We use a kernel  $\phi(\mathbf{x}, \mathbf{y}) = \psi_{6,4}(\|\mathbf{x} - \mathbf{y}\|_2)$  given by the Wendland function  $\psi_{6,4}(r) = (1-r)_+^{10}[25+250r+1,050r^2+2,250r^3+2,145r^4]$  where  $x_+ = x$  for  $x \geq 0$  and  $x_+ = 0$  for  $x < 0$ . The corresponding Sobolev space is  $H^{5.5}(\mathbb{R}^2; \mathbb{S}^{2 \times 2})$ . The grid  $X$  has  $N = 600$  collocation points, black dots in Figure 1. We mark the area where the constraints of Verification Problem fail to be fulfilled; in blue if (VP1) is violated and in red if (VP2) is violated. We used the standard triangulation, cf. (Giesl and Hafstein, 2015), of the area  $[-1.6, 1.6] \times [-1.6, 1.6]$  with  $1500^2$  vertices for the CPA interpolation. In order to obtain a positively invariant set, we computed a Lyapunov-like function solving (11) using RBF and interpolating the solution with a CPA interpolation. We used the same collocation grid  $X$ , but another Wendland function  $\psi_{5,3}(cr)$  with parameter  $c = 0.9$  and a triangulation of  $[-1.65, 1.65] \times [-1.65, 1.65]$  with  $1000^2$  vertices. In the first plot of Figure 2, the failing points for the Lyapunov-like function are marked in yellow and the level set is the curve in green. The periodic orbit is the curve in orange. In the second figure, the level set

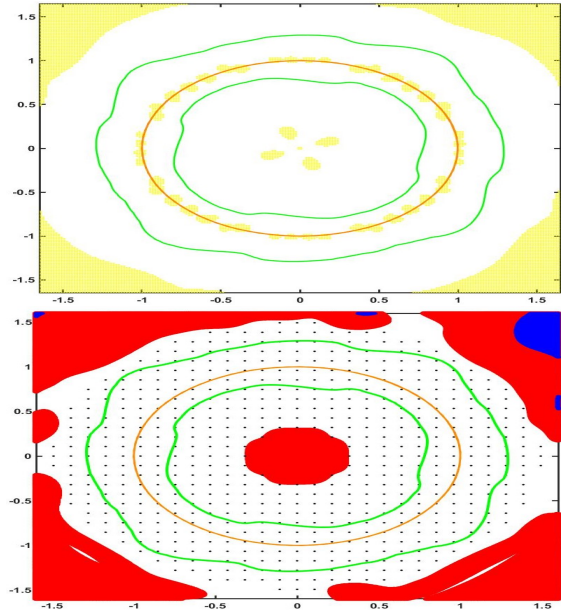


Figure 2: Example 3.1. The orange curve indicates the periodic orbit for system (12). The yellow areas denote the simplices, where the Lyapunov-like function is not decreasing. The green curves are the level set of the Lyapunov-like function, which thus indicate the boundary of a positively invariant set. The second figure shows the positively invariant set (bounded by the green curves), the collocation points (black dots) as well as the blue area, where (VP1) is not fulfilled, and the red area, where (VP2) is not satisfied. The positively invariant set (bounded by the green curves) is thus a subset of the basin of attraction of a unique periodic orbit within it.

of the Lyapunov-like function and the area suggested by our method suitable for the contraction metric are displayed together. Thus, the sublevel set is a subset of the basin of attraction of a unique periodic orbit. We now consider the perturbed system

$$\begin{cases} \dot{x} &= (x+\epsilon)(1-x^2-y^2)-(y+\epsilon) \\ \dot{y} &= (y+\epsilon)(1-x^2-y^2)+(x+\epsilon) \end{cases} \quad (13)$$

with  $\epsilon = 0.2$ . We use the same Lyapunov function and contraction metric as in the unperturbed system. We can see in plots of Figure 3 that both the contraction metric and the Lyapunov-like function computed for the unperturbed system satisfy the constraints for the perturbed system in a very similar area as before.

### 3.2 A Three-dimensional Example

We consider the following three-dimensional system from (Giesl, 2019, Section 5.3)

$$\begin{cases} \dot{x} &= x(1-x^2-y^2)-y+0.1yz \\ \dot{y} &= y(1-x^2-y^2)+x \\ \dot{z} &= -z+xy \end{cases} \quad (14)$$

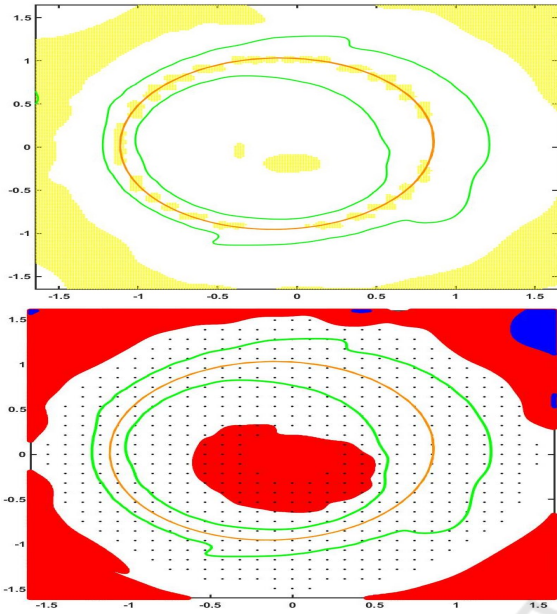


Figure 3: Example 3.1. The orange curve indicates the periodic orbit of the perturbed system (13) with  $\epsilon = 0.2$ . The yellow areas denote the simplices, where the Lyapunov-like function is not decreasing. The green curves are the level set of the Lyapunov-like function, which thus indicate the boundary of a positively invariant set. The second figure shows the positively invariant set (green), the collocation points (black dots) as well as the blue area, where (VP1) is not fulfilled and the red area, where (VP2) is not satisfied. The positively invariant set (bounded by the green curves) is thus a subset of the basin of attraction of a unique periodic orbit within it – note that the contraction metric and Lyapunov-like function have been computed for the unperturbed system, but the conditions are checked for the perturbed system.

which has an exponentially stable periodic orbit.

We choose the parameters of the method in the following way:  $B(\mathbf{x}) = I_{3 \times 3}$  and  $N = 4,458$  collocation points to cover the area  $\{(x, y, z) \in \mathbb{R}^3 : 0.75 < \sqrt{x^2 + y^2} < 1.55, |z| < 0.45\}$  using a hexagonal grid, see (Iske, 1998), and a scaling factor  $\alpha = (0.1398, 0.1398, 0.09)$ , as well as the point  $\mathbf{x}_0 = (1, 0, 0)$  with  $c_0 = 1$ . We use the kernel given by the Wendland function  $\psi_{6,4}$  with parameter  $c = 0.55$ , the corresponding Sobolev space is  $H^6(\mathbb{R}; \mathbb{S}^{3 \times 3})$ . In Figure 4, the black dots are the collocation points, the orange curve is the periodic orbit, the blue surface represents the boundary of area where (VP1) is not satisfied and the red surface is the boundary of area where (VP2) is not fulfilled. We have triangulated the space  $[-1.67, 1.67] \times [-1.67, 1.67] \times [-0.67, 0.67]$  with  $601^3$  vertices.

For the Lyapunov-like function we use the same set of collocation points, and the kernel given by the

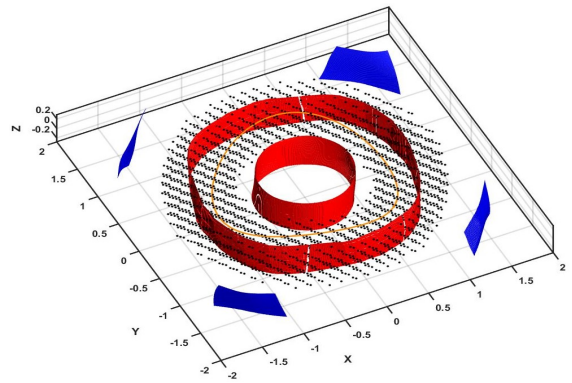


Figure 4: Example 3.2. The orange curve indicates the periodic orbit for system (14). The black dots show the collocation points. The blue surface indicates the boundary of area where (VP1) is not fulfilled. The red surface indicates the boundary of the area where (VP2) is not satisfied.

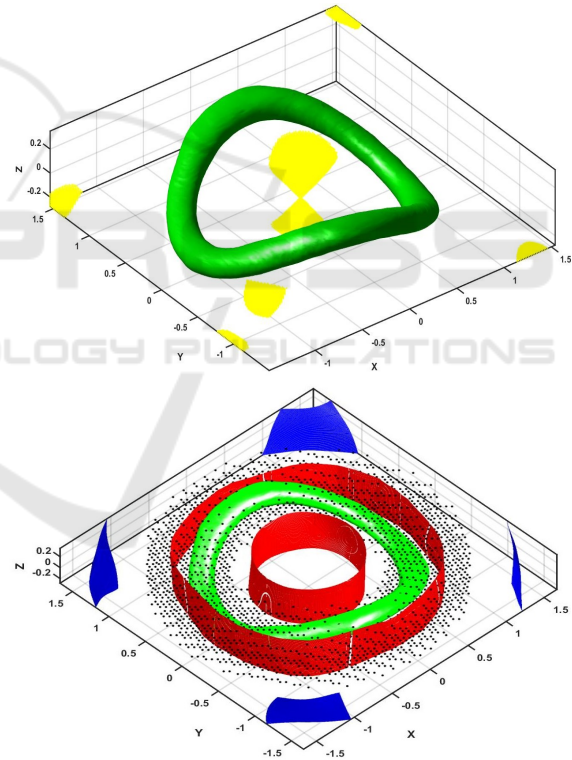


Figure 5: Example 3.2. The area where the Lyapunov-like function, computed for system (14), is not decreasing is plotted in yellow. The green surface is the level set of the Lyapunov-like function, which thus indicates the boundary of a positively invariant set. The second figure shows the collocation points (black dots) as well as the boundary of the area where (VP1) is not fulfilled (blue), and the boundary of the area where (VP2) is not satisfied (red). The positively invariant set (bounded by the green surface in the middle) is thus a subset of the basin of attraction of a unique periodic orbit within it.

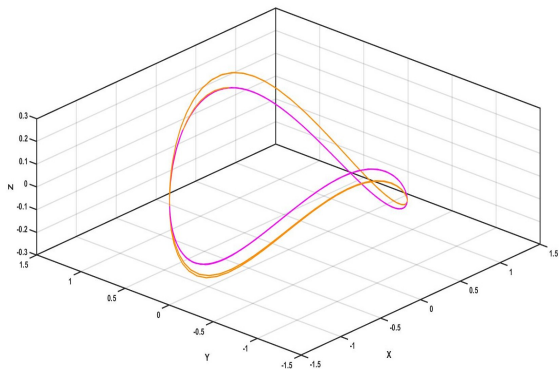


Figure 6: Example 3.2. The periodic orbit for the original system (14) is the curve in magenta, while the periodic orbit for the perturbed system (15) with  $\epsilon = 0.1$  is depicted in orange.

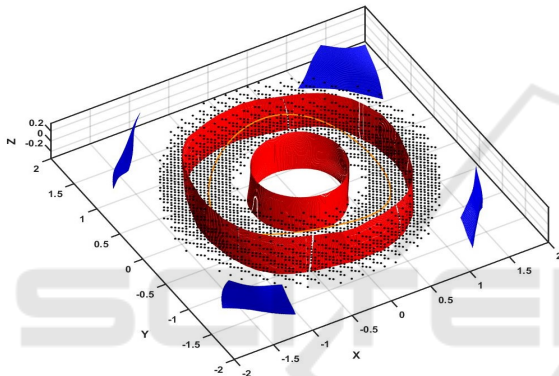


Figure 7: Example 3.2. The contraction metric, computed for the unperturbed system, is checked for the perturbed system: the blue surface shows the boundary of the area where (VP1) fails, while the red surface denote the boundary of the area where (VP2) fails.

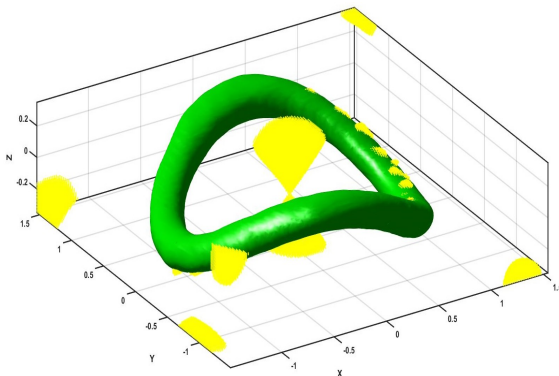


Figure 8: Example 3.2. The Lyapunov-like function for the unperturbed system (14) cannot be used for the perturbed system (15) with  $\epsilon = 0.1$ , because the failing points, where it is not decreasing along solution trajectories, intersects the boundary of the level-set (green).

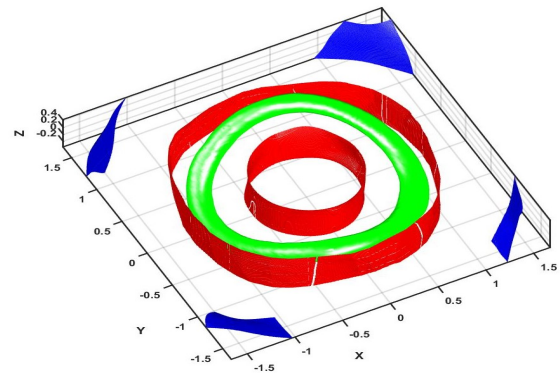


Figure 9: Example 3.2. By computing a new Lyapunov-like function for the perturbed system (15) with  $\epsilon = 0.1$ , we can verify that the area bounded by the green surface is forward invariant. The contraction metric for the unperturbed system can still be used; the boundary of the area where (VP1) is not fulfilled is depicted in blue and the boundary of the area where (VP2) is not satisfied is drawn in red. The positively invariant set (bounded by the green surface in the middle) is thus a subset of the basin of attraction of a unique periodic orbit within it.

Wendland function  $\psi_{5,3}$  with parameter  $c = 0.6$ . In Figure 5, a suitable level set of the Lyapunov-like function is presented in green, while its failing points are in yellow. The second side figure combines all the results, showing that the conditions of the verification problem are satisfied within a compact, and positively invariant set (green).

Now we consider the perturbed system

$$\begin{cases} \dot{x} &= x(1-x^2-y^2) - y + 0.1(y+\epsilon)z \\ \dot{y} &= y(1-x^2-y^2) + x \\ \dot{z} &= -z + x(y+\epsilon) \end{cases} \quad (15)$$

with  $\epsilon = 0.1$ . The periodic orbit for the original (magenta) and perturbed (orange) systems can be seen in Figure 6. It is an interesting observation that while the same contraction metric could be used for the perturbed system, see Figure 7, the Lyapunov-like function fails to give a suitable level set around the periodic orbit and we need to calculate a new one for the perturbed system, see Figure 8.

## 4 CONCLUSIONS

A contraction metric can be used to determine a subset of the basin of attraction of a periodic orbit. Having a PDE characterization of the contraction metric, one can use generalized interpolation with radial basis functions to approximate the solution of the PDE and thus to compute a contraction metric. Subsequently the approximation can be interpolated over a triangulation and it can be rigorously verified that the con-

structured matrix-valued function truly is a contraction metric.

In this paper it was shown, both in theory and examples, that the contraction metric has the advantage of being robust with respect to small perturbations in the system, even those which vary the position of the periodic orbit.

When compared to other methods to determine the basin of attraction of an exponentially stable periodic orbit, e.g. Lyapunov functions, the computation of a contraction metric is computationally more demanding as we construct a matrix-valued function. The advantage is, however, that we do not need the location of the periodic orbit and that the metric is robust with respect to perturbations of the system.

## REFERENCES

- Angeli, D. (2002). A Lyapunov approach to incremental stability properties. *IEEE Trans. Automat. Contr.*, 47(3):410–421.
- Borg, G. (1960). *A condition for the existence of orbitally stable solutions of dynamical systems*, volume 153. Elander.
- Demidovič, B. P. (1961). On the dissipativity of a certain non-linear system of differential equations. I. *Vestnik Moskov. Univ. Ser. I Mat. Meh.*, 1961(6):19–27.
- Demidovič, B. P. (1967). Лекции по математической теории устойчивости. Izdat. “Nauka”, Moscow.
- Forni, F. and Sepulchre, R. (2014). A differential Lyapunov framework for Contraction Analysis. *IEEE Transactions on Automatic Control*, 59(3):614–628.
- Fromion, V. and Scorletti, G. (2005). Connecting nonlinear incremental Lyapunov stability with the linearizations Lyapunov stability. In *Proc. 44th IEEE Conf. Decis. Control*, pages 4736–4741.
- Giesl, P. (2019). Computation of a contraction metric for a periodic orbit using meshfree collocation. *SIAM J. Appl. Dyn. Syst.*, 18(3):1536–1564.
- Giesl, P. (2020). On a matrix-valued PDE characterizing a contraction metric for a periodic orbit. *Discrete Contin. Dyn. Syst. Ser. B*, accepted.
- Giesl, P. and Hafstein, S. (2013). Construction of a CPA contraction metric for periodic orbits using semidefinite optimization. *Nonlinear Anal.*, 86:114–134.
- Giesl, P. and Hafstein, S. (2015). Computation and verification of Lyapunov functions. *SIAM J. Appl. Dyn. Syst.*, 14(4):1663–1698.
- Giesl, P., Hafstein, S., and Mehrabinezhad, I. (2021a). Computation and verification of contraction metrics for exponentially stable equilibria. *J. Comput. Appl. Math.*, accepted.
- Giesl, P., Hafstein, S., and Mehrabinezhad, I. (2021b). Computation and verification of contraction metrics for periodic orbits. *J. Math. Anal. Appl.*, accepted.
- Hartman, P. (1964). *Ordinary Differential Equations*. Wiley, New York.
- Hartman, P. and Olech, C. (1962). On global asymptotic stability of solutions of differential equations. *Trans. Amer. Math. Soc.*, 104:154–178.
- Hauser, J. and Chung, C. C. (1994). Converse Lyapunov functions for exponentially stable periodic orbits. *Systems Control Lett.*, 23(1):27–34.
- Iske, A. (1998). Perfect centre placement for radial basis function methods. Technical Report TUM-M9809, TU Munich, Germany.
- Jouffroy, J. (2005). Some ancestors of contraction analysis. In *44th IEEE Conference on Decision and Control*, page 5450. IEEE.
- Krasovskii, N. N. (1963). *Problems of the Theory of Stability of Motion*. Mir, Moscow, 1959. English translation by Stanford University Press.
- Kravchuk, A. Y., Leonov, G. A., and Ponomarenko, D. V. (1992). A criterion for the strong orbital stability of the trajectories of dynamical systems I. *Diff. Uravn.*, 28:1507–1520.
- Leonov, G., Noack, A., and Reitmann, V. (2001). Asymptotic orbital stability conditions for flows by estimates of singular values of the linearization. *Nonlinear Anal.*, 44(8):1057–1085.
- Leonov, G. A. (2006). Generalization of the Andronov-Vitt theorem. *Regul. Chaotic Dyn.*, 11(2):281–289.
- Leonov, G. A., Burkin, I. M., and Shepelyavyi, A. I. (1996). *Frequency Methods in Oscillation Theory*. Ser. Math. and its Appl.: Vol. 357, Kluwer.
- Lewis, D. C. (1949). Metric properties of differential equations. *American Journal of Mathematics*, 71(2):294–312.
- Lohmiller, W. and Slotine, J.-J. (1998). On Contraction Analysis for Non-linear Systems. *Automatica*, 34:683–696.
- Manchester, I. R. and Slotine, J.-J. E. (2014). Transverse contraction criteria for existence, stability, and robustness of a limit cycle. *Systems Control Lett.*, 63:32–38.
- Opial, Z. (1960). Sur la stabilité asymptotique des solutions d’un système d’équations différentielles. *Ann. Polon. Math.*, 7(3):259–267.
- Rüffer, B., van de Wouw, N., and Mueller, M. (2013). Convergent system vs. incremental stability. *Systems Control Lett.*, 62(3):277–285.
- Stenström, B. (1962). Dynamical systems with a certain local contraction property. *Math. Scand.*, 11:151–155.
- Walter, W. (1998). *Ordinary Differential Equation*. Springer.
- Yang, X. (2001). Remarks on three types of asymptotic stability. *Systems Control Lett.*, 42:299–302.